ARTICLE IN PRESS

Corrosion Science xxx (xxxx) xxx–xxx

Contents lists available at ScienceDirect

Corrosion Science

journal homepage: www.elsevier.com/locate/corsci

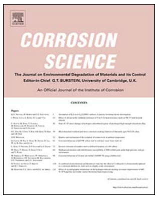

Corrosion behavior and mechanism of 3Cr steel in CO_2 environment with various Ca^{2+} concentration

Bei Wang, Lining Xu*, Guozhang Liu, Minxu Lu

Corrosion and Protection Center, Key Laboratory for Environmental Fracture (MOE), Institute for Advanced Materials and Technology, University of Science and Technology Beijing, Beijing 100083, China

ARTICLE INFO

Keywords:
Low alloy steel
Weight loss
Polarization
Acid corrosion
Passivity

ABSTRACT

The effect of Ca^{2+} on the corrosion behavior of 3Cr steel was investigated using immersion tests and electrochemical measurements. The results demonstrated that with an increase in Ca^{2+} concentration in the solution, the corrosion rate of 3Cr steel decreased and the Ca^{2+} content in the corrosion scale increased. Ca is involved in the formation of both the inner and outer corrosion scales of 3Cr steel. Polarization curves revealed that Ca^{2+} could enhance the pseudopassivation of 3Cr steel. EIS results demonstrated that Ca^{2+} can decrease the porosity of corrosion films. Additionally, Ca^{2+} could accelerate the precipitation of $FeCO_3$ ($Ca_xFe_{1-x}CO_3$) by reducing its solubility and saturation degree.

1. Introduction

In oil and gas fields, Ca^{2+} is commonly present in formation water, and its concentration can be as high as 37,600 mg/kg [1–3]. Numerous studies have demonstrated that Ca^{2+} has a strong effect on corrosion, but such findings are often contradictory. Uhlig et al. [4] indicated that Ca^{2+} additions form diffusion barrier films on carbon steel cathodes. These diffusion barrier films are characterized by an unknown structure that contains both Ca^{2+} and an inhibitor (phosphorus). The presence of Ca^{2+} can substantially improve inhibition. Jiang et al. [1] suggested that Ca^{2+} can delay the initiation of pitting corrosion in N80 steel under stagnant conditions compared with an equal Cl^- concentration. Tavares et al. [5] studied the effect of $CaCO_3$ on the corrosion of low-carbon steel scales in aqueous solution saturated with CO_2 and NaCl at 80 °C and 15 MPa. They indicated that $CaCO_3$ reduced the corrosion rate, but the scales were depassivated and pits then formed during electrochemical measurements. Nesic et al. [6] reported that Ca^{2+} affects corrosion behavior by changing water chemistry; low Ca^{2+} concentration (< 100 ppm) did not significantly affect the corrosion rate, whereas high Ca^{2+} concentration resulted in a high corrosion rate. Wu et al. [7] indicated that Ca^{2+} and ${CO_3}^{2-}$ formed nuclei on the surface of a galvanized steel pipe and grew into spherulites on its corrosion products; the scale slowed the corrosion and the pitting region became smaller. Sridhar et al. [8] reported a synergy between Ca^{2+} and Mg^{2+} in the precipitation of carbonates, and the mixed calcium – magnesium carbonate was discovered to be stable. The effects of Ca^{2+} on the corrosion behavior of pipeline steel can thus not be ignored, even if the findings regarding Ca^{2+} appear to be contradictory.

Low-Cr steel, containing up to 5 wt% Cr, is a new type of steel developed for use in CO_2 environments. Among the low-Cr steels, 3Cr steel has the best combination of cost, being less than 1.5 × more expensive than conventional grades of carbon steel, and CO_2 corrosion resistance, being approximately 3 – 10 × more favorable [9–13]. Numerous studies have been performed to investigate the corrosion resistance mechanisms and scale formation of low-Cr alloy steels [14–18]. Some studies [19,20] have shown that the corrosion scale on 3Cr steel consisted of $FeCO_3$ and $Cr(OH)_3$. Compared with the crystalline corrosion scale of carbon steel, that of 3Cr steel is in amorphous state, which is denser and more protective. Carvalho et al. [21] investigated the corrosion behavior of iron and Fe-Cr alloys (1–5%Cr), and found that small contents of chromium in the alloy decrease the corrosion attack only in very specific pH range $4 < \text{pH} < 5$. Keddam et al. [22,23] proposed a reaction model of the dissolution-passivation process of Fe-Cr alloys on the basis of polarization and EIS experimental results. In the mechanism proposed, the adsorbed species of $FeOH_{ads}$ was maintained to explain the Fe-Cr behavior.

To date, very few studies have addressed the effect of Ca^{2+} on the corrosion behaviors of low-Cr alloy steels. Lu et al. [24] found that the outer scale of weld metal without alloying elements mainly consists of amorphous $FeCO_3$ and $CaCO_3$, and the outer scale of weld metal with alloying elements mainly consists of amorphous $FeCO_3$ and $Cr(OH)_3$. The anions can pass through the amorphous $FeCO_3$ and $CaCO_3$ scale freely, whereas the amorphous $FeCO_3$ and $Cr(OH)_3$ prevent the permeation of anions. Jia et al. [25] studied the effect of Ca^{2+} on the CO_2

---

* Corresponding author.
E-mail address: xulining@ustb.edu.cn (L. Xu).

https://doi.org/10.1016/j.corsci.2018.03.013
Received 16 May 2017; Received in revised form 26 February 2018; Accepted 9 March 2018

Please cite this article as: Wang, B., Corrosion Science (2018), https://doi.org/10.1016/j.corsci.2018.03.013

Table 1
Elemental composition of X65, 3Cr and 6.5Cr steels.

Materials	Element(wt%)									
	C	Si	Mn	S	P	Cr	Mo	V	Nb	Fe
X65	0.05	0.17	1.51	0.005	0.024	/	0.16	0.03	0.04	Bal.
3Cr	0.07	0.20	0.55	0.005	0.005	2.96	0.16	0.03	0.03	Bal.
6.5Cr	0.07	0.20	0.55	0.003	0.003	6.50	0.15	0.03	0.03	Bal.

corrosion of 3Cr steel and discovered $CaCO_3$ to be deposited on the specimen surface, providing protection to the metal substrate. Thus, Ca^{2+} undoubtedly affects the corrosion behavior of low-Cr alloy steels.

Immersion tests and electrochemical measurements were performed in the current study to examine the effect of Ca^{2+} on the corrosion behavior of 3Cr steel. Additionally, this paper is the first to propose the possible mechanism through which Ca^{2+} affects the pseudopassivation of 3Cr steel. It is expected that this research would propel the application of 3Cr steels in the oil and gas fields.

2. Experiment

2.1. Materials and solution

The materials used here were X65, 3Cr and 6.5Cr steels with chemical composition (wt%) listed in Table 1. The specimens (50 mm × 10 mm × 3 mm for immersion tests and 10 mm × 10 mm × 3 mm for electrochemical tests) were ground to 1000 grit, and then cleaned with distilled water and alcohol. The composition and pH value of the test solution, simulating an oil field formation water, is shown in Table 2. Prior to the test, the solution was first deaerated by pure CO_2 for at least 8 h. During the test, the CO_2 gas was continuously bubbled into the solution.

2.2. Immersion tests

The immersion tests were conducted in a 2-L autoclave to investigate the corrosion rate of 3Cr steel in the CO_2 environment. Prior to conducting immersion tests, the original weight (W_0) of each specimen was measured using an analytical balance. After 120 h of immersion, the corroded specimens extracted from the autoclave were immediately rinsed with deionized water and dried. Then the weights (W_1) of specimens with corrosion products were measured. The corrosion products were removed through a chemical cleaning procedure in a solution of 500 mL HCl + 3.5 g hexamethylene tetramine + balanced distilled water for 5 min, rinsed and dried, and then reweighed to obtain the final weight (W_2). The corrosion rate (V_c) was reported in mm/y according to the weight loss calculated using Eq. (1), and the estimated density (ρ_{film}) of the corrosion scale was calculated using Eq. (2),

$$V_c = \frac{876000(W_0 - W_2)}{t\rho A} \tag{1}$$

$$\rho_{film} = \frac{W_1 - W_2}{dA} \tag{2}$$

where W_0 and W_2 are the original and final weight of specimen, g, respectively; t represents the immersion time, h; ρ is steel density, g/cm^3; A is exposed surface area in cm^2; W_1 is the weight of specimen with corrosion products, g; d is the average thickness of corrosion products obtained from cross-sectional morphology, cm.

Table 2
Composition of the test solutions simulating the oilfield formation water.

Composition(mg L^{-1})	NaCl	$CaCl_2$	$NaHCO_3$	pH
1#(0 ppm Ca^{2+})	27740	0	519	5.99
2#(180 ppm Ca^{2+})	27266	450	519	5.90
3#(360 ppm Ca^{2+})	26317	900	519	5.74
4#(720 ppm Ca^{2+})	25368	1800	519	5.69
5#(1080 ppm Ca^{2+})	25318	2700	519	5.68

The morphology and energy dispersive X-ray spectroscopy (EDS) analysis of the corrosion scale were investigated using a JSM-6510A SEM and a JED-2300 EDS.

2.3. Electrochemical measurements

All electrochemical measurements were performed in a 1-L glass cell with a traditional three-electrode system using a Gamry Reference600 electrochemical workstation. Samples of X65, 3Cr, and 6.5Cr steel were used as working electrodes; a platinum sheet was used as a counter electrode, and a saturated calomel electrode (SCE) was used as a reference electrode. The scan rate of the potentiodynamic polarization tests was 0.5 mV s^{-1}. Anodic potentiodynamic polarization measurements were carried out by sweeping the potential from −700 mV to −300 mV (vs. SCE). Cyclic cathodic polarization measurements were carried out with potentials ranging from −700 mV to −1200 mV (vs. SCE). The electrochemical impedance spectroscopy (EIS) measurements were performed at a potential of −550 mV (vs. SCE), after the specimens had been prefilmed through potentiostatic polarization for 1800 s at a potential of −550 mV (vs. SCE). The frequency range was from 100 kHz to 10 mHz. The perturbing AC amplitude was 5 mV.

All tests were performed at 80 °C under stagnant conditions. The immersion tests were conducted at a CO_2 partial pressure of 0.8 MPa. The electrochemical measurements were conducted in CO_2-saturated solution under atmospheric pressure.

3. Results

3.1. Immersion tests

The average corrosion rates of 3Cr steel samples immersed in solutions with different Ca^{2+} concentrations were measured using the weight loss method. As illustrated in Fig. 1, when a constant immersion period of 120 h was used, the corrosion rate decreased with increasing Ca^{2+} concentration.

Fig. 2 displays the micro-morphologies of 3Cr steel after 120 h of immersion. All the corrosion scales on the 3Cr steel specimens in different solutions consisted of two layers. The inner layer, which was flat and intact, was mainly composed of amorphous $FeCO_3$ and $Cr(OH)_3$

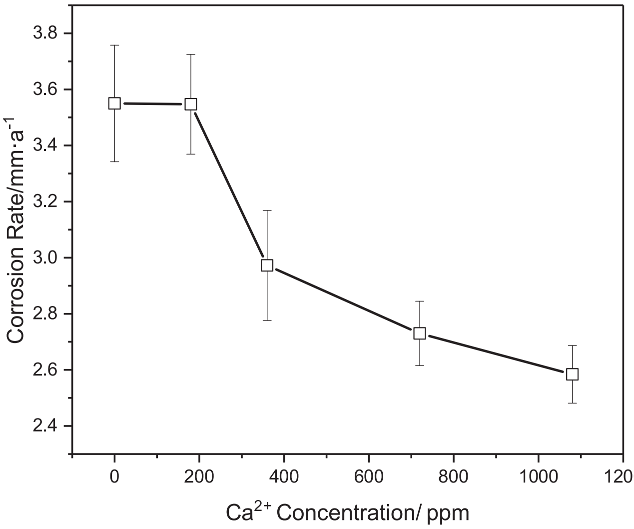

Fig. 1. Average corrosion rates of 3Cr steel in solutions with different Ca^{2+} concentrations.